Calibrating the CORSAIR Polarimeter for its Qualification Flight

Alan Hsu[a], Jenna Samra[b], Steven Tomczyk[c], Daniel Durusky[b], Jacob Hawthorne[b], Vanessa Marquez[b], Abigail Unger[b]

[a] Harvard University, Cambridge, MA, USA, [b] Smithsonian Astrophysical Observatory, Cambridge, MA, USA, [c] Solar Scientific LLC, Boulder, CO, USA

Abstract

We show preliminary results for a probabilistic calibration of the CORSAIR polarimeter. The **COR**onal **S**pectropolarimeter for **A**irborne **I**nfrared **R**esearch (**CORSAIR**) is a new balloon-borne coronagraph and spectropolarimeter that will provide the first uninterrupted observations of the global coronal magnetic field over one month-long solar rotation [1]. We calibrate the polarimeter using a newly developed probabilistic calibration scheme that quantifies the calibration uncertainty explicitly. First, we place a calibration unit in front of the polarimeter to generate known Stokes inputs. Using an infrared source and detector, we project light through the system and record the observed intensities at different modulation states. We model our polarimeter using a probabilistic Mueller matrix framework and initialize prior distributions on free parameters centered on values using point-estimate methods employed by existing polarimeters. We then estimate the posterior distribution of the free parameters, effectively computing the calibration uncertainty in the form of a distribution shift on our initial estimates. **We find that the CORSAIR polarimeter waveplate is consistent with the expected quarter-waveplate behavior, and that the inferred downstream Stokes efficiencies satisfy the system requirements. We also find that field-angle variations in the calibrated parameters across the optic are smaller than the recovered posterior uncertainties.**

Experimental Setup

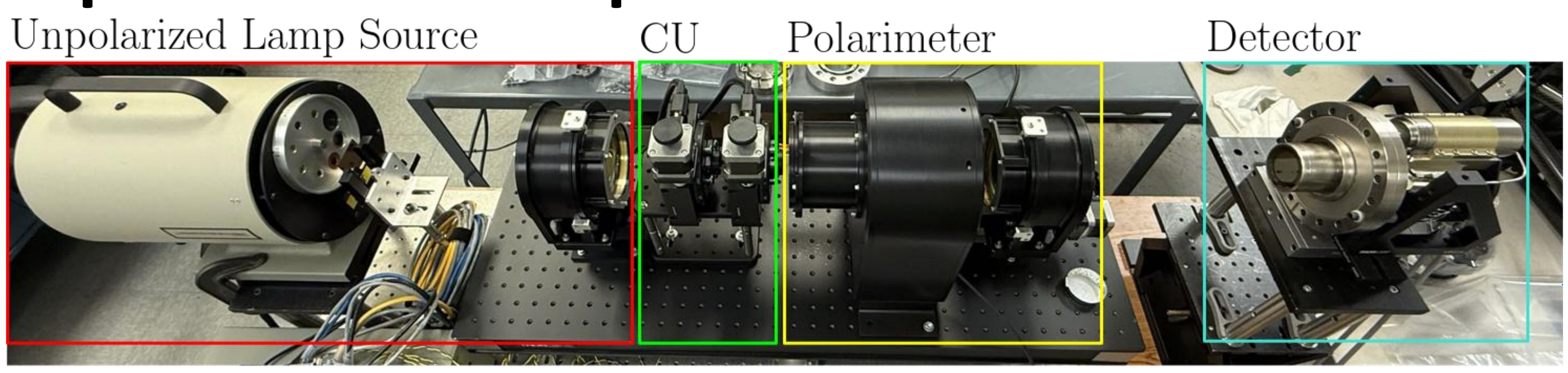

The CORSAIR polarimeter calibration setup. We place an unpolarized lamp source (boxed in red) with a 3.9 micron filter and collimator that produces collimated light at the expected wavelength during actual operation. The light is then fed into a calibration unit (CU, boxed in green) consisting of a linear polarizer (LP) and waveplate (WP) that will generate known Stokes inputs. This is then fed into the CORSAIR Polarimeter (Pol, boxed in yellow) consisting of a WP and LP, and finally focused onto an IR detector (boxed in blue). The CU optics and Pol WP are mounted on automated rotation stages that are programmed to move to desired angles.

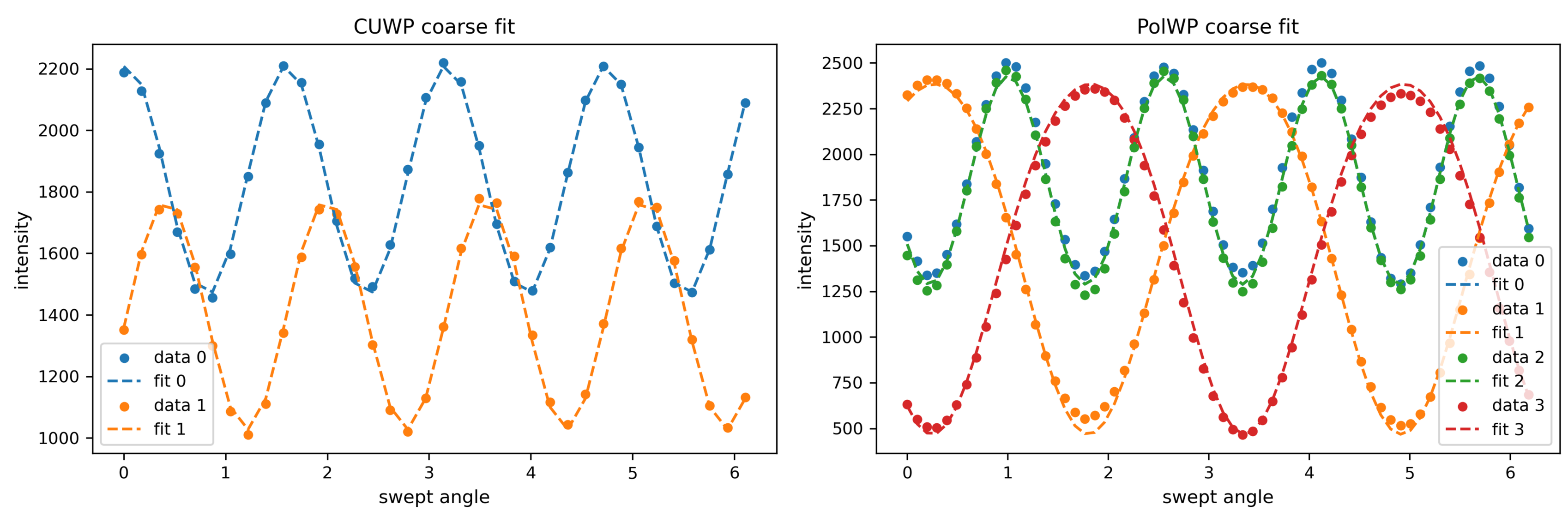

Fits to the collected intensity data using coarse-fitted parameters. The left panel shows the observed intensities of the CU WP coarse dataset and the coarse-fitted sinusoids. The right panel shows the same for the Pol WP coarse dataset and the corresponding coarse-fitted sinusoids. This fit will then be further refined by a Bayesian fine calibration.

Polarimeter Model

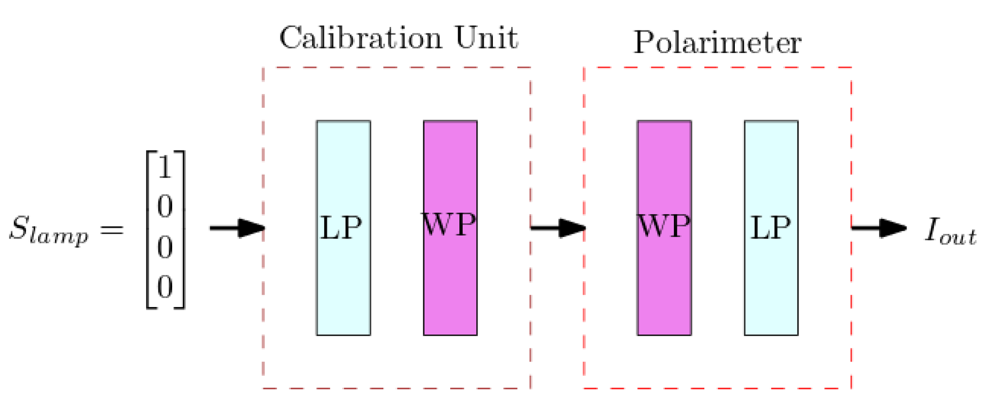

The CORSAIR polarimeter calibration scheme, courtesy of Figure 2 from [2]. We model the CORSAIR polarimeter (Pol) as a Mueller matrix model of a rotating waveplate followed by a linear polarizer. A calibration unit (CU) with an unpolarized source is placed upstream of the CORSAIR polarimeter, consisting of a linear polarizer followed by a waveplate. Calibrating this system amounts to setting the four optics (2 in CU and 2 in Pol) to different states, recording the observed intensities from the detector, and fitting the free parameters in our forward model.

Coarse Calibration

Our calibration pipeline will consist of two parts: a coarse calibration and a fine calibration. The coarse calibration aligns the optics in a common frame (clocking) and provides a coarse, initial guess for the free parameters in our forward model. Key parameters Θ include waveplate retardances, fast-axis locations, and bias and gain values. For fitting the polarimeter waveplate, the intensity data collected are fitted via CMA-ES [3] with the following dataset and objective:

$$\mathcal{C}_{\mathrm{PolWP}} = \{\alpha^m_{c,i}, \theta^m_{c,i}, \theta^m_{p,i}, I_i\}_{i=1}^{N_{\mathrm{PolWP}}}$$

$$\Theta^* = \arg\min_{\Theta} \sum_{\mathcal{C}_{\mathrm{PolWP}}} \left(I(\Theta, \alpha^m_{c,i}, \theta^m_{c,i}, \theta^m_{p,i}) - I_i\right)^2$$

Fine Calibration

Our fine calibration procedure follows the probabilistic formulation of Mueller matrices and the corresponding Bayesian calibration methodology described in [2]. While the coarse calibration determines the global reference frame, the retardance branches of the waveplates, and the coarse-calibrated values of the parameters $\boldsymbol{\omega}$, the fine calibration infers small residual offsets $\boldsymbol{\delta}$ about the coarse solution using a random-state calibration dataset. We assume a Gaussian intensity noise model

$$I_i \sim \mathcal{N}(M(\boldsymbol{\theta}_i, \boldsymbol{\omega}(\boldsymbol{\delta})), \sigma_I^2)$$

which gives the resulting posterior distribution:

$$p(\boldsymbol{\delta}, \sigma_I | \mathcal{C}_{\mathrm{fine}}, \hat{\boldsymbol{\omega}}_{\mathrm{coarse}}) \propto \left[\prod_{i=1}^{N} \mathcal{N}(I_i | M(\boldsymbol{\theta}_i, \hat{\boldsymbol{\omega}}_{\mathrm{coarse}} + P\boldsymbol{\delta}), \sigma_I^2)\right] p_0(\boldsymbol{\delta}, \sigma_I)$$

Bayesian Fine Calibration

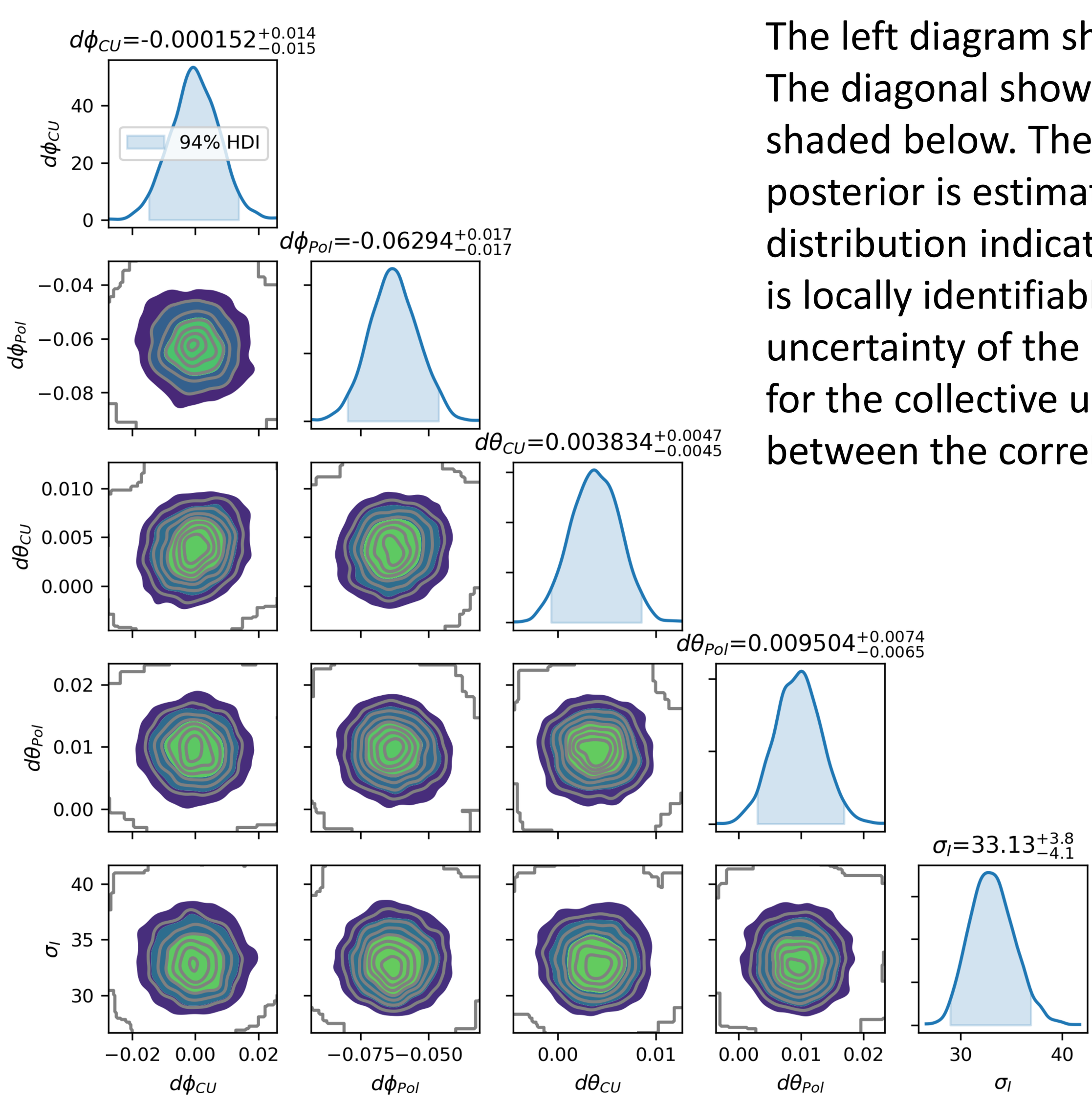

The left diagram shows the corner plot of the posterior for selected fine-fitted parameters. The diagonal shows a KDE of the marginalized posterior distribution (blue), with the 94% HDI shaded below. The off-diagonal plots show pairwise projected posterior distributions. The posterior is estimated using Hamiltonian Monte Carlo (NUTS) samples [4]. The Gaussian-like distribution indicates that the Bayesian calibration produces a well-constrained posterior and is locally identifiable. While one may interpret the HDI interval as an effective calibration uncertainty of the parameters, it is best to view the joint posterior as a representative model for the collective uncertainty across all parameters, as the true uncertainties may leak in between the correlated parameters.

The computed posterior distribution of the parameters can be used to propagate the calibration uncertainties to downstream quantities. The figure below shows the posterior predictive distributions of the Stokes efficiencies given a uniform 8-step polarimeter modulation sequence. In particular, we see that the efficiency for Stokes V is high, which is a nice property for our demodulation matrix to have.

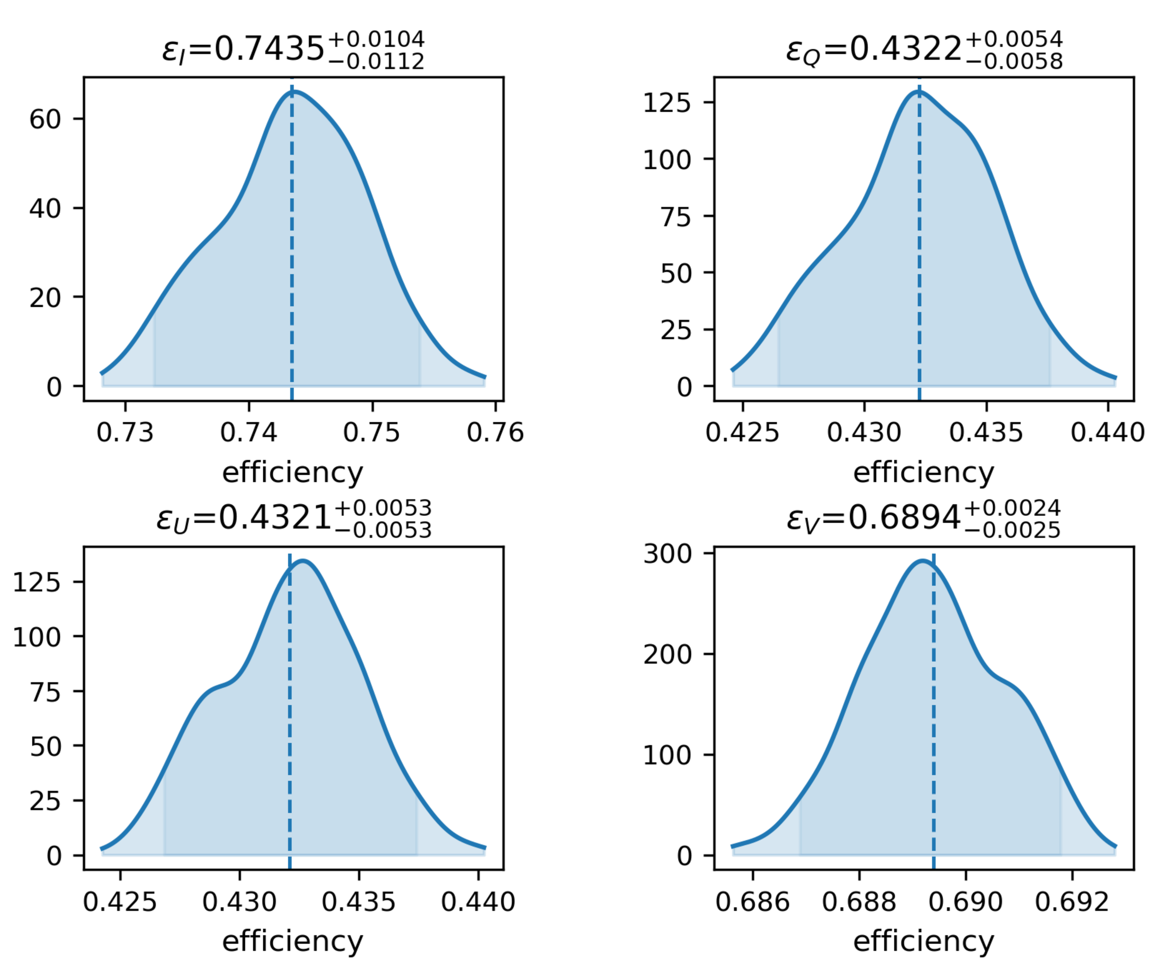

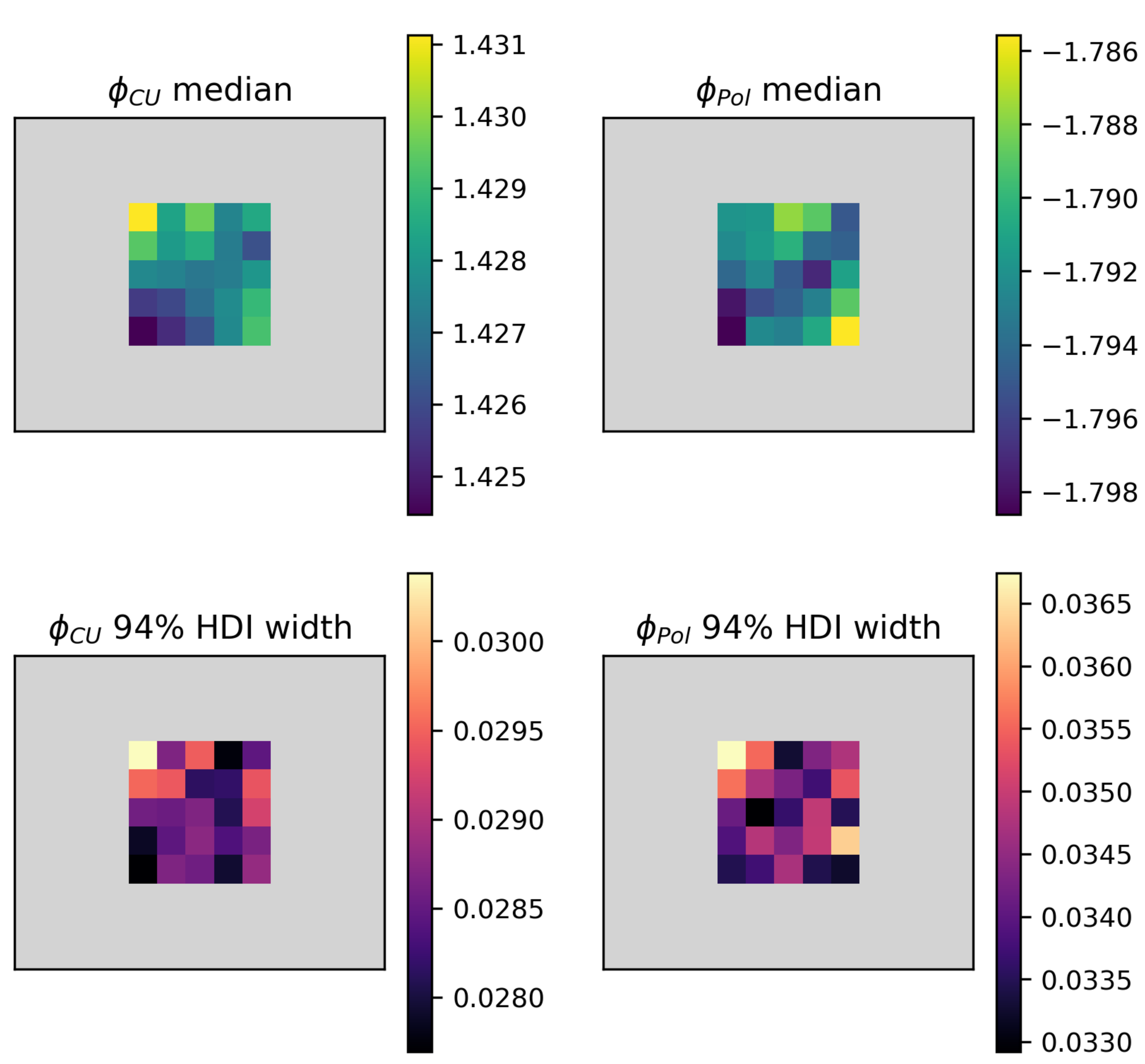

In the left diagram, we extend the coarse and fine calibration procedure to not just one ROI, but a spatial grid of ROIs. We see that the variation in parameters (top row) is less than the posterior uncertainties (bottom row) for the selected waveplate retardance parameters, indicating that there is a weak field-angle dependence. This is a desirable property for coronal observations, since different image pixels probe slightly different field angles through the collimated optics.

References

[1] Samra, Jenna et al. A Balloon-Borne Infrared Coronagraph and Spectropolarimeter for Magnetic Field Measurements of the Solar Corona. 2026 SPIE Astronomical Telescopes + Instrumentation, paper number 14149-67.
[2] Hsu, Alan et al. A Probabilistic Calibration Procedure for the CORSAIR Polarimeter. *Solar Physics*, vol. 301, 41 (2026). https://doi.org/10.1007/s11207-026-02630-4
[3] Hansen, Nikolaus et al. Reducing the time complexity of the derandomized evolution strategy with covariance matrix adaptation (CMA-ES). Evolutionary Computation, 2003 Spring.
[4] Homan, Steven et al. The No-U-turn sampler: adaptively setting path lengths in Hamiltonian Monte Carlo. Journal of Machine Learning Research, vol. 15, January, pp. 1593-1623 (2014).

Contact: alan.hsu@cfa.harvard.edu